J. Membrane Biol. 145, 217–232 (1995)

The Journal of
Membrane
Biology

Small-conductance Chloride Channels in Human Peripheral T Lymphocytes

P.A. Schumacher, G. Sakellaropoulos, D.J. Phipps, L.C. Schlichter
Playfair Neuroscience Unit, The Toronto Hospital Research Institute, 399 Bathurst Street, Toronto, Ontario, Canada M5T 2S8

Received: 17 November 1994/Revised: 7 February 1995

Abstract. During whole-cell patch-clamp recording from normal (nontransformed) human T lymphocytes a chloride current spontaneously activated in >98% of cells (n > 200) in the absence of applied osmotic or pressure gradients. However, some volume sensitivity was observed, as negative pressure pulses reduced the current. With iso-osmotic bath and pipette solutions the peak amplitude built up (time constant ≈23 sec at room temperature), a variable-duration plateau phase followed, then the current ran down spontaneously (time constant ≈280 sec). The anion permeability sequence, calculated from reversal potentials was I^-, Br^- > NO_3^-, Cl^- > $CH_3SO_3^-$, HCO_3^- > CH_3COO^- > F^- > aspartate, gluconate, SO_4^{2-} and there was no measurable monovalent cation permeability. The Cl^- current was independent of time during long voltage steps and there was no evidence of voltage-dependent gating; however, the current showed intrinsic outward rectification in symmetrical Cl^- solutions. The conductance of the channels underlying the whole-cell current was calculated from fluctuation analysis, using power-spectral density and variance-*vs.*-mean analysis. Both methods yielded a single channel conductance of about 0.6 pS at –70 mV (close to the normal resting potential of T lymphocytes). The power spectral density function was best fit by the sum of two Lorentzian functions, with corner frequencies of 30 and 295 Hz, corresponding to mean open times of 0.54 and 5.13 msec. The pharmacological profile included rapid block by external application of flufenamic acid (50 μM), 5-nitro-2-(3-phenylpropylamino)-benzoic acid (NPPB, 100 μM), [6,7-dichloro-2-cyclopentyl-2,3-dihydro-2-methyl-1-oxo-1H-inden-5-yl)oxy] acetic acid (IAA-94, 250 μM) or 100 μM 1,9-dideoxyforskolin. The stilbene derivatives DIDS (4,4′-diisothiocyano-2,2′ disulphonic acid stilbene, 500 μM) and SITS (4-acetamido-4′-isothiocyano-2,2′-disulphonic acid stilbene, 500 μM) prevented buildup of Cl^- current after a 30-min preincubation at 500 μM. When tested in a mitogenic assay, DIDS, flufenamic acid, NPPB and IAA-94 all inhibited T-cell proliferation, suggesting a physiological function in addition to the observed volume sensitivity.

Key words: Whole-cell recording — Anion selectivity — Cl-channel blockers

Introduction

In the past few years, the existence and diversity of anion-selective channels in cell membranes have been increasingly recognized, including a new class of small-conductance (1–2 pS) Cl^- channels that has been described using fluctuation analysis of whole-cell currents. This class comprises Cl^- channels that respond to cell volume (Cahalan & Lewis, 1988; Doroshenko & Neher, 1992; Botchkin & Matthews, 1993; Diaz et al., 1993; Lewis et al., 1993; Stoddard, Steinbach & Simchowitz, 1993) as well as volume-insensitive channels that are activated by second messengers including GTPγS and cAMP (Matthews, Neher & Penner, 1989). Despite these differences in regulation of the small-conductance Cl^- channels, the whole-cell currents have several biophysical features in common; i.e., lack of voltage and time dependence, outward rectification in symmetrical Cl^- solutions, and block by the well known Cl^- transport inhibitor, DIDS (4,4′-diisothiocyano-2,2′ disulphonic acid stilbene), although the extent and voltage dependence of block varied among the cell types.

Roles for Cl^- channels in immune cells have been postulated, but determining their contributions has been hampered by lack of information on channel types and their regulation, lack of selective blockers, and by the rather nonselective nature of most anion channels (i.e.,

Correspondence to: L. Schlichter

permeability to supposedly impermeant anion substitutes). The clearest role for Cl^- channels in T lymphocytes is the restoration of cell volume following an artificially imposed hypotonic shock; i.e., the cells initially swell passively then undergo a regulatory volume decrease (RVD), shrinking back to essentially their original volume (for a recent review, *see* Sarkadi & Parker, 1991). RVD results from the induction of separate conductive pathways for K^+ and Cl^-, net extrusion of KCl and the loss of osmotically obliged water. Candidates for the Cl^- channel include the maxi-conductance channel (*see* Pahapill & Schlichter, 1992*a*) and the small-conductance channel that is the subject of this paper. A second potential role for Cl^- channels is during T-cell activation. Following antibody or antigenic stimulation of T cells via the T-cell receptor, intracellular Ca^{2+} (Ca_i) rapidly rises and remains somewhat elevated for several hours. There is evidence that the sustained Ca_i rise requires high extracellular Cl^- and is blocked by the Cl^--channel blockers, 4-acetamido-4′-isothiocyano-2, 2′-disulphonic acid stilbene (SITS) and DIDS (Rosoff, et al., 1988). Similarly, killing of target cells by cytotoxic T lymphocytes (Gray & Russell, 1986) and by natural killer cells (L.C. Schlichter, *unpublished results*) is inhibited by SITS, DIDS or removal of external Cl^-.

The present study contributes information about activation properties, anion selectivity, pharmacology and possible roles of a prevalent, small-conductance Cl^- channel in normal (i.e., nontransformed), human T lymphocytes. Within 2 sec of establishing a whole-cell recording some Cl^- current was present. The subsequent buildup of Cl^- current did not require hypo-osmotic shock, pressure-induced swelling or addition of ATP to the pipette solution. Current buildup and rundown may result from biochemical events triggered by establishing a whole-cell recording. There appears to be a role for these channels in T-cell activation since several Cl^- channel blockers inhibit the current and inhibit mitogen-induced T cell proliferation at similar doses.

Materials and Methods

Cell Isolation

Human blood was separated and enriched for T lymphocytes by centrifugation on Ficoll Hypaque or on a discontinuous Percoll gradient (both from Pharmacia, Piscataway, N.J.) followed by B lymphocyte and monocyte removal on a nylon wool column for 30 min at 37°C in RPMI 1640 medium with 10% fetal calf serum (Gibco Laboratories, Grand Island, NY). Cell populations obtained in this way were ≥98% T lymphocytes as measured by fluorescence-activated cell sorter (FACS) analysis with the anti-CD3 antibody OKT3 (Ortho Pharmaceuticals, Raritan, NJ). There were no discernible differences in the electrophysiological properties whether cells were washed and resuspended in RPMI for same-day experiments, or resuspended in Aim-V medium (Gibco) and incubated overnight at 37°C with 5% CO_2 for next-day use. Cells were ≥95% viable in all cases as judged by trypan blue exclusion or by a commercial LIVE/DEAD assay (Molecular Probes, Eugene, OR).

Electrophysiology

All patch-clamp recordings were made at room temperature (except as noted in Fig. 5) in the whole-cell configuration using an Axopatch 200 (Axon Instruments, Foster City, CA) patch-clamp amplifier. Pipettes were pulled from borosilicate glass (World Precision Instruments, Sarasota, FL) to resistances of 10–15 MΩ which are higher than normal due to the low ionic-strength pipette solutions used. Our standard pipette solution contained (in mM): 50 n-methyl-d-glucamine chloride (nMDGCl), 1 $MgCl_2$, 0.1 $CaCl_2$, 10 TES (N-tris-(hydroxymethyl) methyl-2-amino ethanesulfonic acid) (Fisher, Fairlawn, NJ), 1.5 EGTA, 120 sucrose and was titrated to pH 7.2 with nMDG. For some selectivity and pharmacology experiments, 50 mM NaCl or 50 mM KCl was substituted for nMDGCl and the pH titrated with NaOH or KOH, respectively. The osmolarity of all pipette solutions was 278–282 mOsm.

For cation substitution experiments, bath solutions contained (in mM): 1 $MgCl_2$, 1 $CaCl_2$, 10 TES, and 140 nMDGCl (or 140 NaCl, KCl or tetraethylammonium chloride, TEACl). These solutions were titrated to pH 7.4 with the hydroxide of the major cation, except for nMDGCl and TEACl, where nMDG was used. A low Cl^- bath solution containing 50 mM nMDGCl and 160 mM sucrose was used for experiments to examine current rectification. The osmolarity of all normal bath solutions was 278–284 mOsm. For anion substitution experiments, the 140 mM NaCl bath solution was substituted by 140 mM of each Na salt, except for Na_2SO_4 where 110 mM was used to maintain normal osmolarity. The following salts were purchased from Sigma (St. Louis, MO): NaI, NaBr, NaCl, $NaHCO_3$, $NaCH_3COO$, Na aspartate. Other Na salts were obtained by titrating the following acids with NaOH: nitric acid (Fisher), gluconic acid (Sigma), hydrofluoric acid (Fluka, Buchs, Switzerland), sulfuric acid (BDH Chemicals, Toronto, Ontario) and methanesulfonic acid (Aldrich, Milwaukee, WI).

Because recordings were begun with standard NaCl saline in the bath, agar bridges were made with 140 mM NaCl saline to reduce the initial liquid-liquid junction potentials. Then, when the bath solution was changed for selectivity studies, junction potentials between solutions were measured in current-clamp mode with a 3 M KCl electrode, and later subtracted from current-versus-voltage (*I-V*) records. For anion selectivity studies, measured junction potentials (140 mM anion, except Na_2SO_4, 110 mM) with respect to 140 mM NaCl saline, were (in mV): I^-, 0; Br^-, 0; F^-, −4; acetate, −6; aspartate, −10; bicarbonate, −8; gluconate, −10; methylsulfonate, −5; NO_3^-, −1; SO_4^{2-}, −9. Junction potentials with respect to 140 mM NaCl saline for cation-substituted solutions were: 140 K^+, −2; 140 TEA^+, +1; 140 $nMDG^+$, +7; 50 $nMDG^+$ bath or pipette solution, −4. All raw records of currents are shown according to electrophysiological convention; i.e., outward currents (upward deflection) corresponding to anions (negative charge) entering the cell. Voltages are reported as intracellular potential with respect to the grounded bath. Command voltages were applied and resultant currents digitized using pClamp software, Ver 5.5.1 (Axon Instruments). Records were filtered at 1 kHz with the four-pole Bessel filter in the patch-clamp amplifier prior to storage on hard disk except for fluctuation analysis, *see* below. Cell (C_c)- and pipette (C_p)-capacitance compensation were performed via the patch-clamp amplifier. Series resistance (R_{series}) was measured for each recording but analogue compensation was not performed, except as indicated in Fig. 1 or when the current was larger than 500 pA. In all cases R_{series} was <25 MΩ hence the largest voltage error (i.e., at +100 mV) is predicted to be 12 mV. Moreover, errors in membrane potential (V_m) due to a voltage drop

across R_{series} vanish as $I_m \rightarrow 0$ pA, therefore the conductance (G_{Cl}) was determined at the reversal potential (E_{rev}) as the slope of a tangent to the *I-V* curve. Digitized *I-V* traces were analyzed using the ClampFit utility of pClamp, then converted to SigmaPlot Ver 4.0 (Jandel Scientific, Corte Madera, CA) files for presentation. All curve fits were performed with TableCurve software Ver 3.1 (Jandel Scientific).

Fluctuation Analysis

For variance-*vs.*-mean and spectral analysis, whole-cell currents were recorded from the moment of break-in until rundown was complete. These currents were low-pass filtered at 10 kHz by the four-pole Bessel filter on the patch-clamp amplifier, played through a pulse-code modulator (PCM-2; Medical Systems, Greenvale, NY), and recorded on VCR (Sony BetaMax) tape. Then, current records were replayed from the VCR tape, low-pass filtered at 3 kHz using an eight-pole Bessel filter (Frequency Devices, Worcester, MA). Fluctuations were separated from the current signal using an eight-pole Butterworth high-pass filter set at 6 Hz, then amplified (10×), low-pass filtered at 3 kHz and digitized at 6 kHz using fluctuation analysis software (Dr. John Dempster, University of Strathclyde, Glasgow, Scotland). Background noise was estimated as the variance (or power spectrum) at E_{rev} or after the current had completely run down. Either value, when subtracted from variance-*vs.*-mean pairings (or current spectrum) via the software, yielded the same result. Variance and mean were calculated for 170 msec-long segments (1024 points/segment) for the duration of buildup (≈80 sec), for a total of 470 segments. Similarly, the power spectral density was calculated during ≈80 sec at the plateau phase, when the current was relatively stationary; i.e., 470 segments of 170 ms each were averaged. R_{series} in series with C_c is expected to behave as a low-pass filter with cutoff frequency (f_c), where $f_c = 1/(2\pi R_{series} C_c)$. Uncompensated R_{series} values during whole-cell recording did not exceed 25 MΩ, and C_c for T cells is ≈1 pF. These values correspond to a roll-off at ≈6 kHz, well above the 3 kHz cutoff frequency used for analysis. Therefore, estimates of variance and single-channel conductance were not affected by filtering artifacts inherent to the recording configuration.

Solutions and Drugs

Salts, buffers and the mitogen, phytahemagglutinin (PHA) were purchased from Sigma (St. Louis, MO). Pipette solutions were made fresh each day or frozen in 1 ml aliquots and thawed on the day of use. Solution osmolality was measured using a freezing-point depression osmometer (model 3MO, Advanced Instruments). Stock solutions of Cl-channel blockers were prepared as follows: DIDS and SITS (Sigma) were prepared as 10 mM stock solutions in 100 mM $KHCO_3$; gadolinium (Gd^{3+}, 10 mM) and diphenylamine sulfonic acid (500 mM) (both from Sigma) were dissolved in distilled water; 9-anthracene carboxylic acid (9-AC, 500 mM), diphenyl carboxylic acid (DPC, 500 mM), furosemide (500 mM), flufenamic acid (500 mM) and 1,9-dideoxyforskolin (100 mM) were obtained from Sigma and dissolved in DMSO; 5-nitro-2-(3-phenylpropylamino)-benzoic acid (NPPB, 500 mM) and [6,7-dichloro-2-cyclopentyl-2,3-dihydro-2-methyl-1-oxo-1H-inden-5-yl)oxy] acetic acid (IAA-94, 500 mM) were obtained from Research Biochemicals (RBI, Natick, MA) and dissolved in DMSO. Verapamil (50 mM) was purchased from Sigma and dissolved in methanol.

Bath exchanges during ion-selectivity or ion-channel blocker studies were performed using a unidirectional peristaltic pump connected to the bath with polyethylene tubing. The volume of perfusate used was 2–4 times that of the bath and rendered a complete solution exchange. This was verified by changes in junction potentials measured with a 3M KCl electrode in the bath, by washout of a dye from the bath or by changes in E_{rev} for K^+ currents.

Proliferation Assay

Polymorphonuclear (PMN) cells were isolated from freshly drawn human blood (provided by Dr. G. Downey, Department of Medicine, University of Toronto) or from buffy coats obtained from the Red Cross blood bank. 2×10^5 cells were placed in each well of a 96-well plate and incubated with the mitogenic lectin, phytahemagglutinin (PHA, 5 μg/ml, Sigma) in 200 μl of RPMI-1640 cell culture medium containing 2 mM L-glutamine, 10 μg/ml gentamicin and 10% (v/v) heat inactivated fetal bovine serum (all from Gibco). Cultures were maintained at 37°C in a humidified, 5% CO_2 atmosphere for a total of 72 hr. Fifteen hours before harvesting the cells, 0.5 μCi of ^{3}H-thymidine (Amersham, Oakville, Ontario, Canada) was added to each well. Cells were lysed with distilled water then harvested onto glass filtermats using a Skatron cell harvester (Sterling, VA). Proliferation was expressed as counts per minute (cpm ± SEM, n = 6 experiments, 3 replicates/experiment) of ^{3}H-thymidine incorporated into cellular DNA, as detected by liquid scintillation counting using a Beckman LS 8000 β counter and CytoScint scintillation cocktail (ICN, Aurora, OH).

Statistics

Where appropriate, results are expressed as mean ± SEM with the number of cells or experiments in parentheses. The Students' *t*-test was used to test for significant differences and $P < 0.05$ is taken to be significant.

Results

Expression of the Current is Transient

In order to isolate whole-cell Cl^- currents, Na^+ and K^+-free solutions containing $nMDG^+$ were used, except as noted in Figs. 3 and 6. Figure 1 shows that the recent history of the membrane potential does not affect the whole-cell conductance; i.e., the lack of time dependence justifies the subsequent use of a voltage ramp protocol as a true measure of chord and slope conductances over a wide voltage range. We conclude that the channels underlying this whole-cell current are active over a wide voltage range and do not show time-dependent activation or inactivation kinetics. Because the current was outwardly rectified despite having symmetrical Cl^- across the membrane, rectification is not due to differing ion availabilities across the membrane, but appears to be an intrinsic property of the channel. We ruled out the possibility that rectification of current was caused by the pH buffer, TES, which is largely anionic at physiological pH, since either omitting TES and using bicarbonate/CO_2-buffered internal and external solutions, or substituting the pH buffer, HEPES, did not change the rectification.

Within ≈90 sec of establishing the whole-cell configuration ("break-in") under control conditions at room

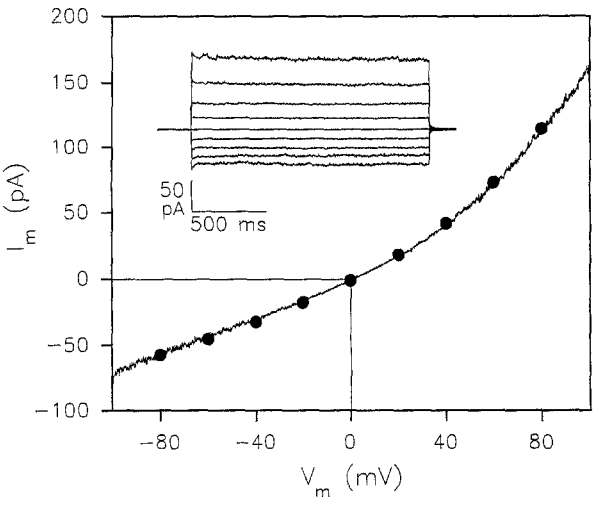

Fig. 1. The outwardly rectifying whole-cell current can be studied using voltage steps or ramps. Inset: Voltage (V_m) steps were applied at 20 – mV intervals between −80 and +80 mV from a holding potential (V_h) of 0 mV. Note the lack of time-dependent kinetics at any V_m, and the presence of outward current rectification. Then a 2-sec long voltage ramp from −100 to +100 mV was applied immediately after the step protocol. Resulting ramp currents are superimposed on currents from voltage steps (filled circles) measured 1 sec into each step. The good agreement between ramp and step data confirms the lack of time-dependence to this current. Solutions were 50 mM nMDGCl in the bath and pipette. All current-*vs.*-voltage traces have been corrected for junction potential offsets (*see* Materials and Methods).

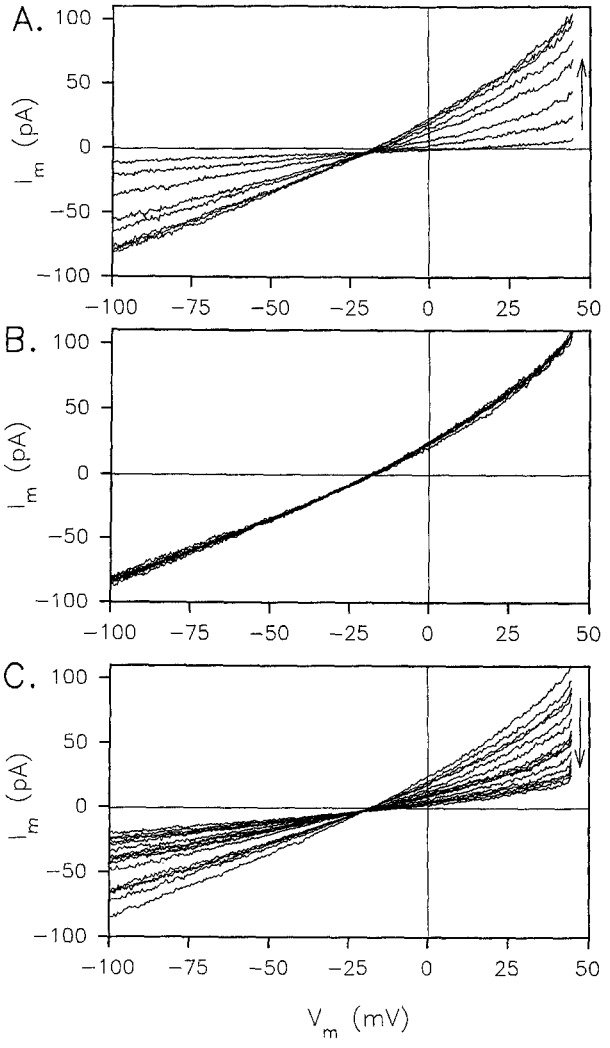

Fig. 2. The current builds with time after break-in, reaches a quasi-stationary plateau, then runs down. Applying 2-sec long ramps of V_m from −100 to +50 mV every 10 sec, starting immediately after break-in, G_{Cl} (defined in text) increased monotonically during the first 6 traces (*A*), stabilized at a constant peak value for 10 traces (*A* and *B*), then ran down during the following 15 traces (*C*). Solutions were 140 mM nMDGCl saline bath and 50 mM nMDGCl pipette solution.

temperature, a whole-cell current developed to a 100–400 pA peak at +50 mV, reached a quasistationary plateau (>1 min), then ran down over several minutes (*shown* under Figs. 2 and 5). To permit the continual monitoring of reversal potential (E_{rev}) and whole-cell conductance (G_{Cl}) over a wide voltage range, the membrane potential (V_m) was ramped from −100 to +50 mV every 10 sec starting immediately upon break-in. Between ramps, V_m was held at −25 mV ($\approx E_{Cl}$ with 140 mM nMDGCl saline in the bath and isosmotic 50 mM nMDGCl pipette solution). Figure 2 shows the resultant currents from a representative cell at room temperature (≈24°C). There was little current during the first ramp, essentially only a nonselective leak, which reversed at 0 mV. Over the following 90 sec, the conductance built to a peak (buildup; Fig. 5*A*), remained roughly constant for ≈80 sec (plateau; Fig. 5*B*), then diminished within 3–4 min (rundown; Fig. 5*C*).

Anion Selectivity

The reversal potential of the current suggested a Cl^- selective channel since E_{rev} was −21 mV for 52 mM internal Cl^- and 144 mM external Cl^- (Fig. 2), which is close to the theoretical equilibrium potential for Cl^- (E_{Cl} = −26 mV) as predicted by the Nernst equation and E_{rev} was ≈0 mV in symmetrical Cl^- (Fig. 1). Further proof the current is carried by Cl^- is as follows: The only elemental ions present in these solutions were Ca^{2+}, Mg^{2+}, H^+/OH^- and Cl^-, with corresponding Nernst potentials at room temperature of +145 mV, 0 mV, −12 mV, and −26 mV, respectively. Moreover, E_{rev} was −56 mV with 155 mM extracellular Cl^- and 16 mM intracellular Cl^- (*data not shown*). As shown in Fig. 3*A*, in the presence of small cations the whole-cell current retained a high Cl^- selectivity. Other inorganic and some organic anions can also permeate the Cl^- channel. Figure 3 shows *I-V* relations and the Table summarizes the results for 11 anion species. For the Table, anion selectivity was determined from reversal potentials and from whole-

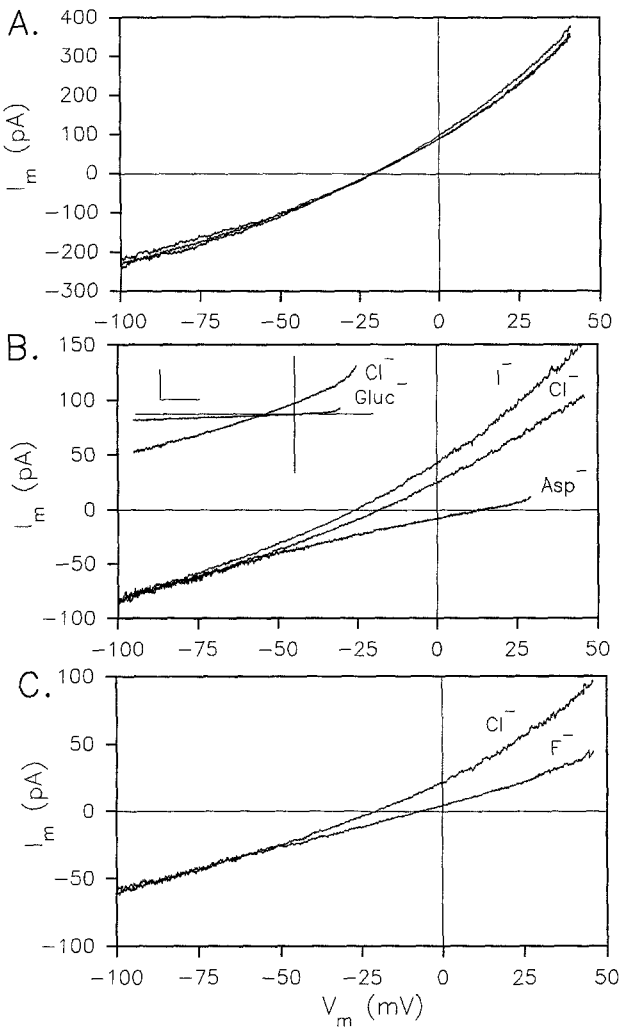

Fig. 3. The current is anion selective. The command voltage (V_m) was ramped from −100 to +50 mV at a time when the conductance was at its plateau (*see* text). The pipette solution was 50 mM nMDGCl throughout. (*A*) Cation substitutions do not affect the amplitude or reversal potential (E_{rev}). The bath initially contained 140 mM nMDGCl saline which was then exchanged with 140 mM NaCl, then KCl, then TEACl saline between ramps. (*B* and *C*) The current shows selectivity among anions. Between ramps the original 140 mM NaCl in the bath solution was substituted by 140 mM of the Na salt of each anion. Three different cells are shown. E_{rev} values in this figure are: I, −26 mV; Cl^-, −21 mV; F, −5 mV; aspartate, +14 mV; gluconate, +15 mV. Average values of E_{rev} were used to calculate relative permeabilities (shown in the Table) from a modified Goldman-Hodgkin-Katz equation:

$$P_X/P_{Cl} = \frac{(a_{Cl})_{0,1} \cdot \exp[-FJ_{GHK}/(RT)] - (a_{Cl})_{0,2}}{(a_X)_{0,2}}$$

where J_{GHK} is the difference between the reversal potential measured in Cl^-/Cl^- solution compared with that in X^-/Cl^- solution. Junction potentials were subtracted (*see* Materials and Methods). The degree of dissociation of the weak acids at pH 7.4 was taken into account, and ion activities were calculated from corresponding activity coefficients (Robinson & Stokes, 1959); i.e., for external Cl^- before and after bath exchange ($(a_{Cl})_{0,1}$ and $(a_{Cl})_{0,2}$ and for anion *X* after bath exchange ($(a_x)_{0,2}$).

Table. Anion Selectivity

Anion	E_{rev} ± (mV) SEM	γ_x/γ_{Cl}	P_x/P_{Cl}
I^-	−25 ± 1	1.11	1.17
Br^-	−25 ± 1	1.11	1.17
NO_3^-	−22 ± 2	1.03	1.04
Cl^-	−21 ± 2	1.00	1.00
$CH_3SO_3^-$	−18 ± 1	0.83	0.89
HCO_3^-	−18 ± 1	0.78	0.89
CH_3COO^-	−5 ± 1	0.67	0.52
F^-	−1 ± 1	0.56	0.44
Aspartate	+14 ± 1	0.44	0.24
Gluconate	+15 ± 2	0.39	0.23
SO_4^{2-}	+13 ± 2*	0.39*	0.23

* To balance osmolarity, $[SO_4^{2-}]_o$ was 110 mM, instead of 140 mM as with all other anions. E_{rev} and γ_x/γ_{Cl} for SO_4^{2-} should therefore not be directly compared to those of the other ten anions. P_x/P_{Cl} for SO_4^{2-} was calculated from the GHK current equation. Slope conductances were calculated at E_{rev}.

cell conductance ratios, since these two measures do not always yield the same sequence. Except for different anions in the bath solution, all solutions were otherwise identical, including the additional 4 mM extracellular Cl^- contributed by 1 mM $CaCl_2$ and 1 mM $MgCl_2$. Hence we have determined the selectivity among different anions from bi-ionic conditions in which the internal Cl^- was always ≈52 mM. Ion interactions within the pore could affect the measured reversal potentials, such that permeability might depend on whether the test anion is added to the inside or outside membrane face. For example, a test anion might reduce the whole-cell conductance if it blocks channels or increase the conductance if it prolongs channel openings.

The P_x/P_{Cl} values in the Table were calculated from the difference in E_{rev} between 140 mM extracellular Cl^- and complete substitution with test anion, calculated by reformulating the GHK equation to an equivalent form (*see* Fig. 3 legend). In theory, the shape of the *I-V* relation following complete substitution of the extracellular anion can give information about channel block or gating changes caused by that anion. That is, the conductance ratio for the anion (γ_x/γ_{Cl}) may not be the same as the permeability ratio (P_x/P_{Cl}). As a first approximation, chord conductances were calculated between −90 mV (predominantly Cl^- efflux) and +30 mV (predominantly test anion influx); however, a complicating factor was noted. When external SO_4^{2-}, aspartate, and gluconate were perfused in, the inward current decreased quickly after bath exchange, that is, at negative potentials where Cl^- efflux dominates (*see* Fig. 3*B* inset, where inward current was eliminated by gluconate). This is consistent with a voltage-dependent block by bulky anion species either from the outside or after they enter the cell. For this reason, the slope conductances reported for these anions in the Table were calculated at E_{rev} from the first

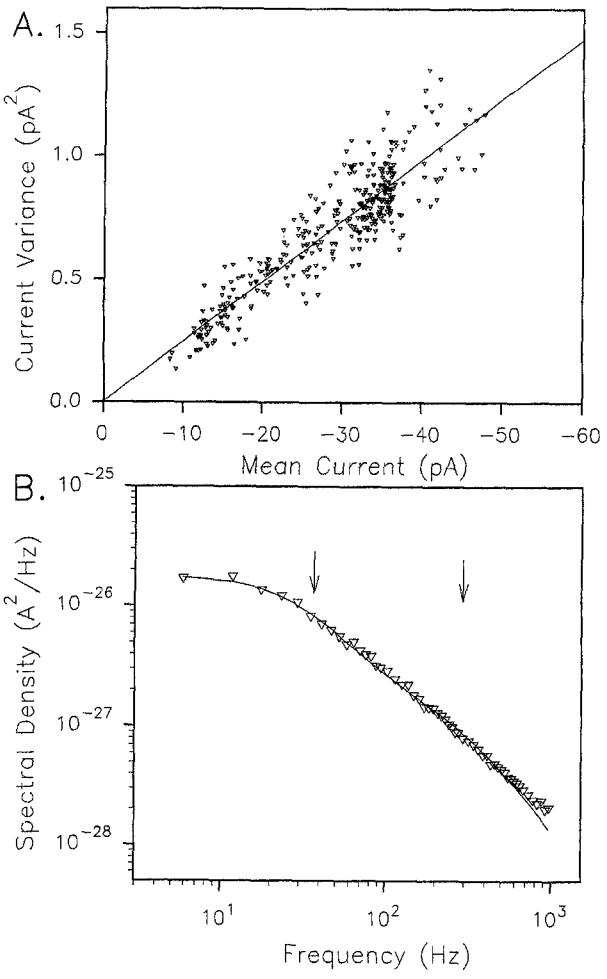

Fig. 4. Estimating the single-channel properties from fluctuation analysis. Current from a representative cell was recorded during buildup and rundown then background noise subtracted (*see* Materials and Methods). Bath solution, 140 mM nMDGCl saline; pipette solution, 50 mM nMDGCl saline. (A) Variance-*vs.*-mean (σ^2 *vs.* I_m) pairings were calculated at $V_m = -70$ mV from 470 segments of 170 msec each during buildup of the current. According to binomial theory, for N independent channels, each with a stationary open probability (P_o) during each segment, and conducting a current i_c while open,

$$\sigma^2 = i_c \cdot I_m - \frac{I_m^2}{N}$$

thereby relating σ^2 to I_m, i_c, and N. The solid curve is the fit of the data to $\sigma^2 = i_c I_m$. The estimated single-channel conductance was 0.63 pS, with $N \approx 1700$ active channels calculated for this cell. (B) Power spectral density (PSD) plot of the current at the plateau from the same cell as above (V_m, −70 mV). The best fit was a double Lorentzian function of the following form:

$$S(f) = S_1(0)/1 + (f/f_{c1})^2) + S_2(0)/(1 + (f/f_{c2})^2)$$

where $S(f)$ is the PSD at frequency f. Corner frequencies are indicated by the arrows at 30 Hz and 295 Hz and variance, $S_i(0) = 1.63 \times 10^{-26}$ A^2/Hz and $S_2(0) = 1.40 \times 10^{-27}$ A^2/Hz. From this fit the variance (σ^2) was calculated and the single-channel amplitude (i_c) estimated as 0.03 pA at −70 mV (conductance, 0.63 pS).

I-V trace during perfusion, immediately after E_{rev} had settled to its new value but before the apparent onset of block (*see* Fig. 3*B* current with aspartate in the bath). Because of possible channel block and the unknown sidedness of this effect we cannot make too much of the exact magnitude of organic anion conductances; however, the conductance and permeability sequences were the same. Our main findings are: (i) several physiologically relevant anions can permeate (Cl^-, NO_3^-, HCO_3^-; (ii) some anions used as nonpermeant Cl^- substitutes in physiological experiments may permeate (e.g., gluconate, methylsulfate); and (iii) the selectivity sequence among halides (I^-, $Br^- > Cl^- \gg F^-$) is similar to Eisenman's Sequence I (Diamond & Wright, 1969), consistent with anion permeability being a function of the ease with which the extracellular anion is dehydrated. The halide selectivity ($I^- > Cl^- \gg F^-$) is the same as we observed in single-channel recordings of the large, multiple-conductance, "maxi"-Cl channel in these human T lymphocytes (Schlichter et al., 1990).

Single-Channel Properties

The smoothness of the whole-cell current traces (*see* Figs. 1–3), indicated that the single-channel conductance underlying this current is small. Accordingly, in extensive cell-attached and excised-patch studies of the maxi-Cl channel in human T cells, no small-conductance Cl^- channel was seen (Schlichter et al., 1990; Pahapill & Schlichter, 1992*a*). The conductance of the Cl^- channel underlying the current in the present study was deduced through the analysis of fluctuations in whole-cell currents. Because the whole-cell conductance changed relatively slowly with time at the plateau and during buildup at room temperature, it was possible to sample segments of current that were stationary for the duration of each segment. Consequently, the current variance (σ^2) and mean (I_m) could be calculated for each segment (*see* Fig. 4 legend), yielding as many σ^2 *vs.* I_m pairings as the number of segments. A straight-line ($\sigma^2 = i_c \cdot I_m$) fit the data much better (F statistic = 2000) than the parabolic fit from the full equation in the figure legend (F statistic = 1000). This implies that P_o was <0.1, since the full equation strictly applies only for $P_o > 0.1$; i.e., the current variance produced by channels opening and closing decreases when channels remain open. The scatter plot of the data in Fig. 4*A* yields the estimate, $i_c = 0.03$ pA. The driving force was 48 mV ($V_m - E_{rev}$), so the single-channel conductance ($g_{Cl} = 0.03$ pA/48 mV) was 0.63 pS. This small g_{Cl} value means that typical whole-cell Cl^- currents in human T cells are mediated by thousands of single channels.

Further estimates of the single-channel conductance and of the mean open time of the channel were obtained by analyzing the power spectral density function (PSD).

From a stationary duration of current during the plateau phase, current fluctuations were fast-Fourier transformed and plotted in the frequency domain (Fig. 4*B*). Estimates of single-channel amplitude (i_c) using this approach rely on the assumption that the probability of opening (P_o) is low (i.e., $1\text{-}P_o \approx 1$). This assumption is reasonable (*see above*) since the variance-*vs.*-mean data were best fit by a straight line (Fig. 4*A*) and the estimated single-channel conductance of 0.63 pS was the same using both types of analysis. At the opposite extreme; i.e., larger channels with $P_o = 1$ a white noise spectrum would have resulted (Johnson or shot noise through open channels) in a flat power spectral density plot. Moreover, discrete jumps of current were never observed during buildup or rundown of current and the current variance was directly proportional to the mean current (Fig. 4*A*). The corner frequencies (f_{c1}, f_{c2}) at which the power of each Lorentzian function was half-maximal were used to calculate the mean channel open times. The mean open times (5.13 msec and 0.54 msec) most likely reflect channel-like behavior with underlying stochastic openings and closings, rather than transporter or pumplike behavior.

Properties of Buildup and Rundown of Current

We first examined more quantitatively the time course of buildup and rundown of the Cl^- conductance. To do this, the instantaneous slope conductance (G_{Cl}) was determined at E_{rev} by fitting a third-order polynomial to current traces from voltage ramps, then differentiating and solving for $V_m = E_{rev}$. This equation was chosen as the one that consistently yielded excellent fits to the voltage-ramp data ($r^2 > 0.999$ in all cases). Figure 5*A* shows the evolution of G_{Cl} with time after break-in at room temperature. For each cell (n = 10) the G_{Cl} value at each time point was normalized to the peak G_{Cl} for that cell, then averaged over all ten cells. The resultant average G_{Cl} values were again normalized, to give the average Cl^- conductance as a function of time, expressed as a fraction of the peak value. In this way, error bars reflect variability associated with the time course of conductance changes, rather than variability in absolute conductance between cells. For the purpose of quantifying the kinetics of these conductance changes, the following definitions are employed. The plateau is defined as the period during which G_{Cl} does not fall more than 5% below its peak value. As shown in Fig. 5*A*, both the buildup and rundown were well fit by monoexponential functions with time constants of ≈23 sec and 280 sec, respectively (*see* equations in figure legend).

We then examined whether changes in intracellular Cl^- (Cl_i) due to diffusional exchange with the pipette filling solution were likely to account for the observed changes in conductance. This possibility seemed unlikely since we had previously estimated the Cl_i concentration as 40–50 mM (i.e., similar to the pipette solution), based on reversal potentials for large conductance Cl^- channels in cell-attached patches (Pahapill & Schlichter, 1992*a*). Consistent with this expectation, Fig. 5*B* shows that during the entire process of current buildup, plateau and rundown, E_{rev} remained near E_{Cl}, even when G_{Cl} was very low and E_{rev} was contaminated by leak; i.e., early on in the buildup or late in the rundown. Figure 5*B* shows the average E_{rev} (open circles) for the same cells and on the same time scale as in Fig. 5*A*.

It has been reported that whole-cell Cl^- currents mediated by small-conductance channels may rundown if ATP is omitted from the pipette-filling solution (Lewis et al., 1993). In contrast, including 4 mM ATP in the pipette solution (added from a frozen stock solution of ATP) had no effect on the rate of buildup or rundown, or on the peak conductance attained (Fig. 5*C*). We had previously found that increasing the temperature to physiological levels dramatically increased the activation and inactivation rates for the voltage-dependent K^+ channels in these cells. Similarly, results in Fig. 5*C* show significantly faster buildup and dramatically faster rundown at 37°C compared with room temperature.

Because the buildup and rundown of Cl^- current were well described by monoexponential functions, we addressed the question of whether these processes are likely to represent diffusional exchange of molecules other than Cl^- or ATP between the pipette and the cell cytoplasm. Cloning and expression studies have demonstrated a molecule (called pI_{Cln}) that was originally thought to be a Cl^- channel (Paulmichl et al., 1992). This molecule now appears to be a cytoplasmic regulator of an endogenous swelling-activated Cl^- channel in *Xenopus* oocytes (Krapivinsky et al., 1994). Diffusion of a solute (e.g., pI_{Cln}) from the pipette into the cell may be considered with a simple one-compartment model, assuming the concentration in the pipette (c_p) is constant, and the concentration throughout the cell (c_c) is uniform, so that the only concentration gradient exists across the pipette tip. For progressively smaller cells with simple geometric shapes (e.g., spherical T lymphocytes, 7 μm diameter), these assumptions become reasonable. The intracellular concentration (c_c) is then given by:

$$c_c(t) = c_p + (c_o - c_p) \cdot e^{\frac{\rho D}{R_p V} \cdot t} \quad (1)$$

(Mathias, Cohen & Oliva, 1990), which is a monoexponential relaxation between c_o and c_p with time constant $R_p V/\rho D$, where ρ is the electrical conductivity of the saline and D is the diffusion coefficient. The validity of this simple model for $c_c(t)$ after break-in was tested for human T cells using the voltage-activated K^+ current ($I_{K(V)}$) as an indicator (Fig. 6). $I_{K(V)}$ can be activated by voltage steps immediately upon break-in, and its voltage- and time-dependence are well known (e.g., Pahapill &

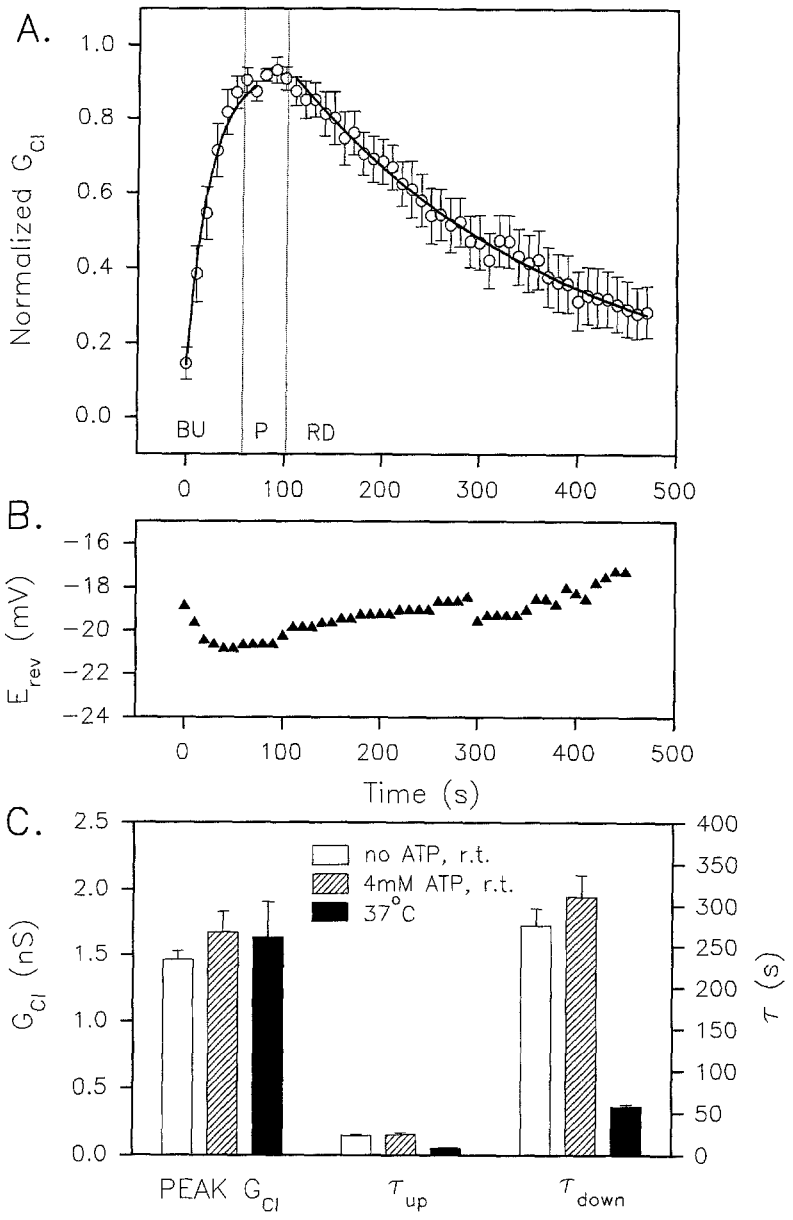

Fig. 5. Properties of the spontaneous buildup and rundown of the Cl^- current. (*A*) After entering the whole-cell recording configuration at $t = 0$, there was a buildup (*BU*) of Cl^- conductance (G_{Cl}) measured as slope conductance of the *I-V* relation at E_{rev} (*see* text). The time course of G_{Cl} changes (mean ± SEM, n = 10) was well-described by a monoexponential function between G_{Cl} at $t = 0 (G_o)$ and the first data point during the plateau ($G_{pl,f}$):

$$G_{Cl}(t) = G_{pl,f} + (G_o - G_{pl,f}) \cdot e^{-t/\tau_{up}}$$

The time constant for the buildup phase, $\tau_{up} = 22.8$ sec. Following the quasi-stationary plateau (*P*), G_{Cl} rundown (*RD*) was similarly well-described by a monoexponential function between the last data point in the plateau ($G_{pl,l}$) at time $t_{pl,l}$ and the final G_{Cl} value in the rundown (G_f):

$$G_{Cl}(t) = G_f + (G_{pl,l} - G_f) \cdot e^{-(t-t_{pl,l})/\tau_{down}}$$

The time constant for the rundown phase, (τ_{down}) was 276 sec. (B) During buildup and rundown of the current, there was very little change in reversal potential, E_{rev}. Mean values for the same 10 cells as in *A* plotted as a function of time after break-in (error levels are ± 1 mV throughout). (*C*) Buildup and rundown are accelerated at 37°C but unaffected by the presence of ATP in the pipette. With 4 mM K_2ATP in the pipette (n = 8), there was no significant difference ($P = 0.1$) in mean peak G_{Cl}, τ_{up}, or τ_{down} values compared with normal pipette solutions (n = 10). In contrast, τ_{up} and τ_{down} at 37°C (n = 4) were significantly shorter than at 24°C (n = 10, $P < 0.001$ in both cases); however, there was no significant difference ($P = 0.1$) in peak G_{Cl} values at these two temperatures. Solutions were 140 mM nMDGCl saline bath and 50 mM nMDGCl pipette solution.

Schlichter, 1990, 1992*b*). To enhance the K^+ current and reduce the Cl^- current the bath solution was 140 mM KAsp saline and the pipette solution 50 mM KAsp saline, chosen for the low permeability of aspartate. V_m was stepped from −90 to +50 mV to activate the K^+ current, then ramped from +50 to −90 mV to determine E_{rev}. This voltage protocol was performed every second starting at break-in to monitor the time course of E_{rev} changes and resultant K^+ currents are shown in Fig. 6*A*. As the intracellular K^+ concentration ($[K^+]_i$) fell from its initial value to the pipette concentration ($[K^+]_p$) of 50 mM, E_{rev} shifted from +4 mV to +24 mV. Using the Nernst equation, $[K^+]_i(t)$ was calculated from $\Delta E_{rev}(t)$, the difference between E_{rev} at time t ($E_{rev}(t)$) and its final value, $E_{rev}(t_\infty)$:

$$[K^+]_i(t) = [K^+]_i(t_\infty) \cdot e^{\left\langle \frac{-zF\Delta E_{rev}(t)}{RT} \right\rangle} \quad (2)$$

This approach circumvents errors in estimating $[K^+]_i(t)$ from $E_{rev}(t)$ due to a shunting of E_{rev} from E_K towards 0 mV by a nonspecific leak. From Eq. (2), setting $c_p = [K^+]_p$, $c_c(t) = [K^+]_i(t)$ and $c_o = [K^+]_i(0)$, and rearranging, gives

$$\ln([K^+]_i(t) - [K^+]_p) = \frac{\rho D}{R_p V} \cdot t + \ln([K^+]_i(0) - [K^+]_p) \quad (3)$$

The fit of Eq. 3 to the plot of $\ln\{[K^+]_i(t) - [K^+]_p\}$ *vs.* t is shown in Figure 6*B*, and yields estimates of $-\rho D/R_p V = 0.31$/sec and $[K^+]_i(0) = 117$ mM. R_p, measured from a

series of experiments was 25 ± 5 MΩ (n = 10) and ρ, measured for the pipette solution was 121 ± 2 Ω · cm (n = 8) and the volume of a T cell is $180 \cdot 10^{-12}$ cm^3 (spherical, 7 μm diameter cell). The calculated diffusion coefficient (D) for K^+ is $1.15 \cdot 10^{-5}$ cm^2/sec, a value about 40% slower than K^+ diffusion in dilute aqueous solutions; i.e., $1.96 \cdot 10^{-5}$ cm^2/sec. Then, using the average τ_{up} = 22.8 sec (from Fig. 5*A*) and a single-compartment model, we calculated a diffusion coefficient for the hypothetical inhibitory factor of $0.16 \cdot 10^{-5}$ cm^2/sec, about 14% as fast as the rate of K^+ diffusion from the cell. Although this is a reasonable diffusion coefficient for a small molecule, several of our observations suggest that neither the buildup or rundown of Cl^- current results only from the diffusional loss of regulatory factors from the cell inhibitor. This is addressed by data shown in Fig. 5 where the effect of raising the bath temperature was investigated. Cell-attached recordings were begun at room temperature (≈24°C), then the bath temperature was raised to 37°C prior to break-in. Figure 5*C* shows the time course of normalized G_{Cl} buildup and rundown from cells at 37°C *vs.* 24°C controls. Both buildup and rundown were dramatically accelerated at 37°C, such that the quasi-stationary plateau observed at room temperature was absent; i.e., τ_{up} and τ_{down} at 37°C (8.2 ± 0.8 sec and 58.3 ± 3.0 sec, respectively) were significantly shorter than at 24°C (22.8 ± 1.7 sec and 276 ± 18.4 sec; $P < 0.01$, Student's t-test). In addition, the mean normalized G_{Cl} at break-in at 37°C (0.49 ± 0.12) was significantly larger than at 24°C (0.15 ± 0.04; $P < 0.01$), suggesting that the Cl^- conductance in the intact cell is significantly higher at physiological temperature. Maximal G_{Cl} values were not significantly different at 37°C. We have obtained a similar result for the large-conductance Cl^- channel in cell-attached patches (Pahapill & Schlichter, 1992*a*), wherein the probability of opening dramatically increased with temperature.

As described above, if τ_{up} is due simply to a diffusive event, it will be inversely proportional to the diffusion coefficient (D) of the (unknown) diffusing particle. The observed decrease in τ_{up} by about one third upon raising the bath temperature would then correspond to a threefold increase in the value of D. However, by the Nernst-Einstein relation $D = k \cdot T/f_s$ (where k is Boltzmann's constant and f_s is the molecular frictional coefficient), so D is directly proportional to absolute temperature (T). Raising T from 24°C (297 K) to 37°C (310 K) should cause only a ≈4% increase in the value of D. The observed acceleration of current buildup at 37°C is much too large to be due to an increased rate of diffusion, arguing that G_{Cl} buildup itself is not a reflection of a diffusive loss of an inhibitory factor. Alternatively, most biochemical processes are significantly slower at room temperature than at 37°C. The accelerated buildup of current at 37°C may reflect an increase in the activity of some enzyme(s) (e.g., protein kinase) underlying channel

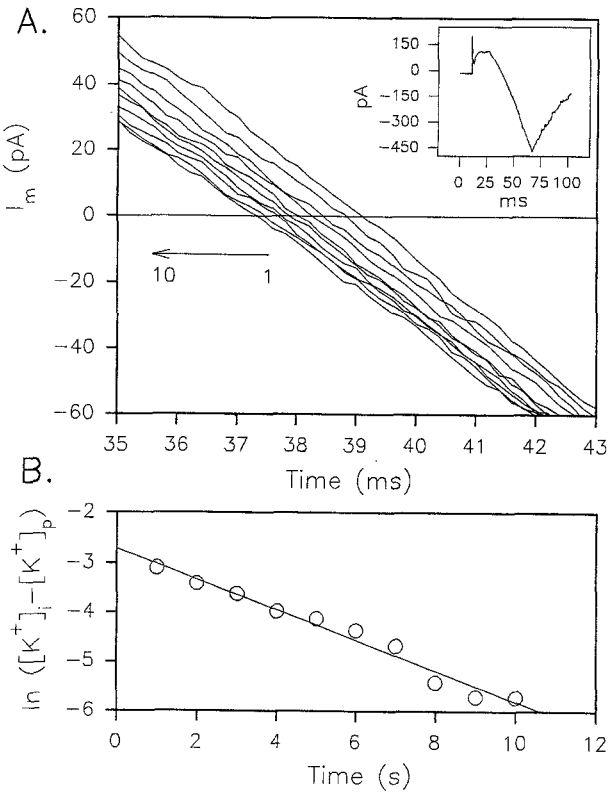

Fig. 6. Estimating the diffusion coefficient for K^+ from the time course of changes in E_K after break-in. (*A*) Starting 1 sec after break-in and repeated every second thereafter, V_m was stepped for 20 ms to +50 mV to activate K(V) channels, then ramped during 40 ms down to −90 mV. (The inset shows the resulting current during one trial). The current-*vs.*-time traces during 10 successive ramps are shown on an expanded scale. The zero current values (E_{rev}) shifted from +4 mV during the first trace to +24 mV by trace 10. (*B*) $[K^+]_i$ at time t was calculated from E_{rev} values (*see* text accompanying Eqs. 1–3). The straight line fit of Eq. 3 to the plotted data has slope 0.31/sec, corresponding to a diffusion coefficient (D) for K^+ of $1.15 \cdot 10^{-5}$ cm^2/sec. Solutions were 140 mM KAsp saline bath and 50 mM KAsp pipette solution.

activation. This is also consistent with a larger G_{Cl} in the intact cell, as estimated by G_{Cl} immediately after break-in at physiological temperature. Since the process underlying G_{Cl} buildup is well-described by a single exponential, it may reflect a one-way, single-step reaction, whose rate constant, k_f would be the inverse of the exponential time constant τ_{up}. Rearranging the Arrhenius rate equation and substituting $\tau_{up} = 1/k_f$,

$$E_{act} = R \cdot \ln \left\langle \frac{\tau_{up,1}}{\tau_{up,2}} \right\rangle \cdot \left\langle \frac{T_1 T_2}{T_2 - T_1} \right\rangle \quad (4)$$

where E_{act} is the Gibbs free energy of activation and $\tau_{up,i}$ is τ_{up} at $T = T_i$ $\{i = 1,2\}$. From the above data, the estimate of E_{act} is 60.2 kJ/mol. Our conclusion from these calculations is that the buildup of G_{Cl} is not due to a simple diffusive event, but that it probably reflects the rate of a chemical process initiated upon break-in.

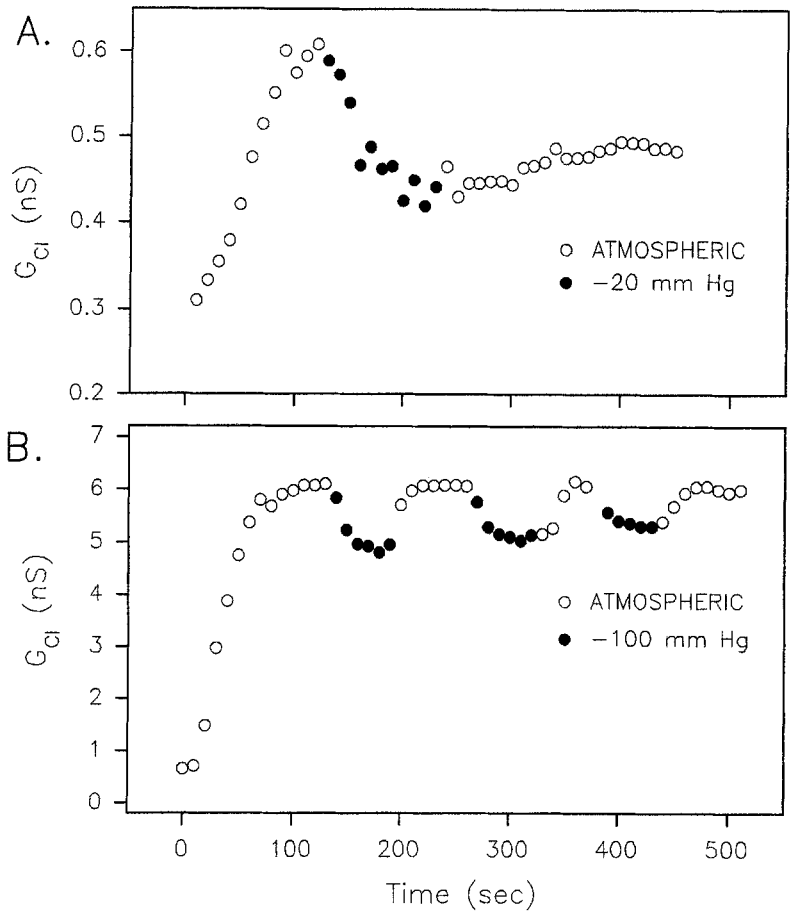

Fig. 7. G_{Cl} can be reduced by applying negative pressure to the pipette to shrink the cell. (*A*) After normal G_{Cl} buildup in iso-osmotic solutions at atmospheric pressure (open symbols), accelerated rundown was induced by −20 mm Hg intracellular pressure (filled symbols). Return to atmospheric pressure failed to restore G_{Cl}. Similar results were seen in 8/10 cells. (*B*) Occasionally, much larger spontaneously developing currents were observed (5 out of >200 cells) and in 2/2 cells tested the current recovered after negative pressure pulses were applied. In this cell repeatedly applying −100 mm Hg negative intracellular pressure pulses (filled circles) caused a 20% reduction in G_{Cl}. G_{Cl} rebounded to its peak upon each return to atmospheric pressure (open circles). Solutions were 140 mM nMDGCl saline in the bath, and 50 mM nMDGCl pipette solution.

Volume Sensitivity

Several reports on small-conductance Cl^- channels indicate that they either require cell swelling to activate them or that the conductance is increased by cell swelling (Cahalan & Lewis, 1988; Doroshenko & Neher, 1992; Botchkin & Matthews, 1993; Diaz et al., 1993; Lewis et al., 1993; Stoddard et al., 1993). In the present study, the Cl^- current activated spontaneously in almost every cell (>98% or >196/>200 cells) despite identical osmolarity pipette and bath solutions and similar osmolarities to studies from other laboratories (e.g., Lewis et al., 1993). We attempted to test whether exposure to hyperosmotic solutions before breaking into the whole-cell configuration would prevent current buildup. However, despite trying different degrees of hyper-osmolarity, different durations of exposure and a variety of pipette shapes and sizes we were unable to break into cells under these conditions. If a hyperosmotic solution was applied after breaking into the cell it appeared to be too late; once the current started to build, it continued. Hence, to test for swelling activation we applied positive pressure to the pipette (up to +100 mm Hg) and observed dramatic swelling (using confocal microscopy) but no increase in peak G_{Cl} (*not shown*). In contrast, applying negative pressure to the pipette decreased the cell volume and decreased G_{Cl} by 20–35% (Fig. 7). Then, restoring the pipette to atmospheric pressure allowed the cell volume to recover but in most cases (8/10) the current did not recover (Fig. 7*A*). During pressure application, there was no evidence for significant changes in series resistance as judged by no change in reversal potential and no change in the capacitance transients during voltage jumps at the beginning and end of each ramp. For the two cells in which the current recovered and negative pressure could be reapplied, G_{Cl} was unusually large before pressure manipulations (e.g., Fig. 7*B*). This may reflect biochemical regulation of the channel since we have recently found conditions that increase the current amplitude (GTPγS or cAMP in the pipette, Schlichter, Schumacher & Sakellaropoulos, 1994).

Ion-Channel Blockers

Several channel blockers known to affect Cl^- channels in lymphocytes and other cell types were tested. In addition, we tested gadolinium (Gd^{3+}) which inhibits regula-

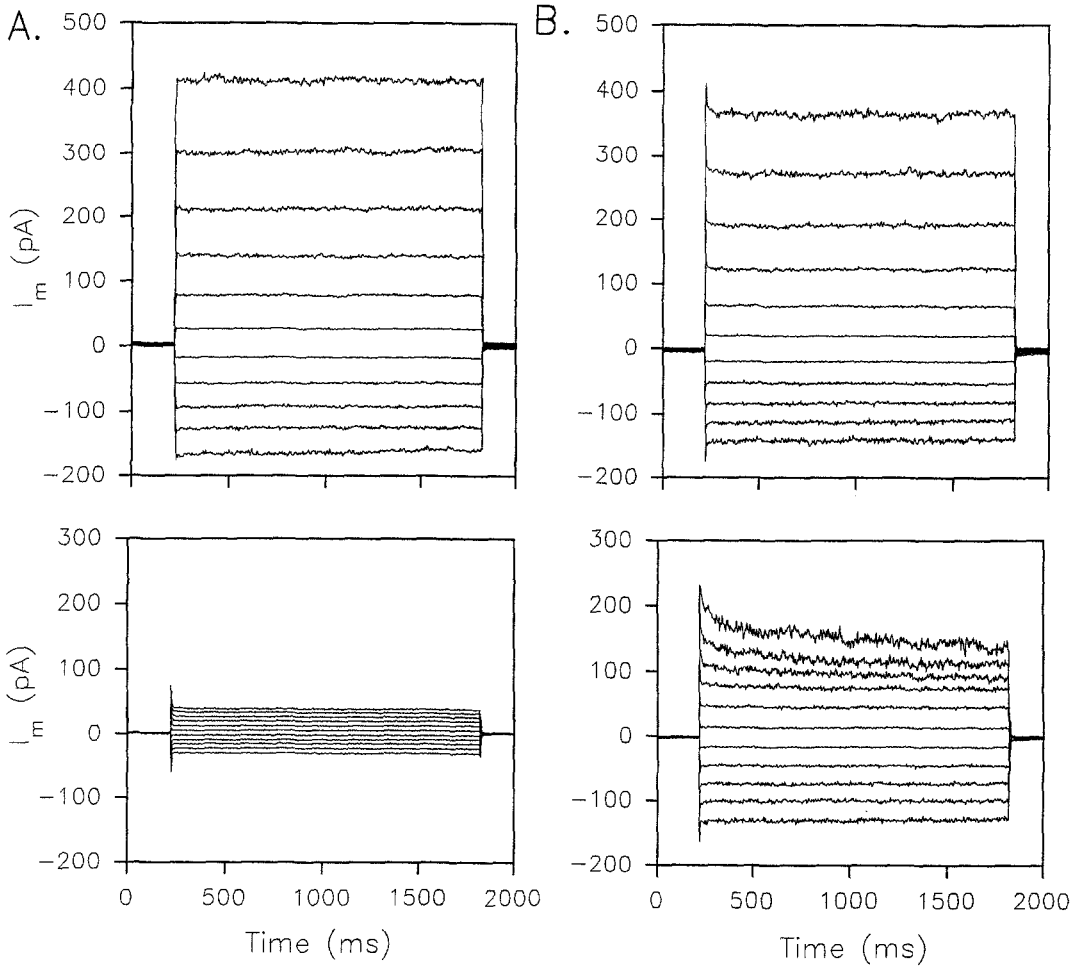

Fig. 8. Blockers of the Cl^- current. (*A*) Flufenamic acid blocks the current in a time- and voltage-independent manner. Control recording during the long-lasting plateau phase. From a holding potential of −10 mV, V_m was stepped from −100 to +100 mV in 20-mV increments at 2-sec intervals. Below—Within 20 sec after addition of 50 μM flufenamic acid to the bath the Cl^- current was blocked, then the voltage-step protocol was started. Solutions were 140 mM nMDGCl saline bath, and 50 mM nMDGCl pipette solution. (*B*) Acutely applied DIDS weakly blocks the Cl^- current, and only at positive potentials. Above—control recording from a different cell, same protocol as *A*. Below—Cl^- currents during voltage steps with 500 μM DIDS in the bath, beginning 1 min after drug addition. Note the time course of the onset of block at +100 mV, and the absence of block at negative potentials.

tory volume decrease (RVD) in T cells (Deutsch & Lee, 1988). In experiments to test for acute channel block, effects of external drug application could easily be dissociated from spontaneous current rundown at room temperature. Each cell acted as its own control and each drug was applied as soon as the peak current was attained; i.e., when three successive voltage ramps produced the same current amplitude. Then, channel block was assessed within 1 min. To determine if block was voltage dependent, voltage steps were applied as shown in Fig. 8, in which case a complete experiment (control, channel block) required ≈2.5 min. At this time, in untreated cells at room temperature, 50–90% of maximal current remained (*see* Fig. 5*A*).

No block of the Cl^- current was observed following acute exposure to as high as 1 mM Zn^{2+} (n = 6), 100 μM 9-AC (n = 4), Gd^{3+} (n = 22) or DPC (n = 5), or 500 μM furosemide (n = 3), acetazolamide (n = 4), or diphenylamine sulfonic acid (n = 4) (*data not shown*). However, as shown in Fig. 8*A*, 50 μM flufenamic acid blocked the Cl^- current within 1 min of bath exchange, in a voltage-independent manner. Complete channel block was obtained in 9/9 cells at 50-100 μM; however, at 10 μM or less, the onset of block by flufenamic acid was slow and difficult to distinguish from current rundown, making interpretation problematic. Acute treatment with 500 μM DIDS resulted in very little block of the current (Fig. 8*B*) and similar results were obtained with SITS (*data not shown*). For both SITS (n = 3) and DIDS (n = 6), block was enhanced slightly at very positive potentials. Because inhibition of RVD in human T cells by SITS, DIDS or Gd^{3+} requires preincubation with drug and high

concentrations of SITS or DIDS (500–1000 μM, *see* Sarkadi & Parker, 1991) we determined if prolonged exposure to these drugs might be required for the onset of block. Cells were incubated for 30 min with 500 μM SITS or DIDS or 50μM Gd^{3+} prior to patch clamping. No G_{Cl} buildup was observed following a 30-min preincubation with SITS or DIDS, in the continued presence of these drugs (6/6 cells), whereas all 5 control cells had >300 pA current at +100 mV. Hence, SITS and DIDS preincubation prevented the spontaneous development of Cl^- current. In contrast, after a 30-min preincubation and in the continued presence of 50 μM Gd^{3+}, no decrease in peak G_{Cl} (5/5 cells) was observed (*data not shown*).

For two well known Cl^- channel blockers (NPPB, and IAA-94, Landry et al., 1989; Matthews et al., 1989; Valverde et al.; 1992; Diaz et al., 1993) we tested acute, external block as above and block by internally applied drugs (*see* Fig. 9). For internal block, drugs were added to the pipette-filling solutions and populations of control cells (no drug) were compared with treated cells from the same blood donor on the same day by alternating control cells with treated cells. Using this protocol we found that 250 μM IAA-94 (10/10) or 100 μM NPPB (13/13) caused a complete (95 ± 5%) and rapid block of the Cl^- current when applied from the outside. After block of Cl^- current the remaining current appeared to be a nonselective leak; i.e., with a linear *I-V* curve reversing at about 0 mV and no sign of time or voltage dependence. Figure 9 (left-hand panels) shows typical examples of acute, external block within 20 sec after application of 250 μM NPPB (*A*) or 250 μM IAA-94 (*B*). Then, because washing for up to 5 min did not restore the current (first ≈2 min shown) we asked whether block was due to drug permeation into the cell and channel block from the inside. The right-hand panels of Fig. 9 show that the initial Cl^- current amplitude was normal with either 250 μM NPPB (*A*) or IAA-94 (*B*) present in the pipette, but the same concentrations of these drugs added to the bath solution rapidly and completely blocked the current (NPPB, n = 4; IAA-94, n = 3). Verapamil (100–250 μM) had no effect on the Cl^- current when added to the bath (8/8 cells) or to the pipette (4/4 cells). In contrast, 100 μM bath applied 1,9-dideoxyforskolin (DDF) eliminated the Cl^- current within 2 min (9/9 cells). After full block (96 ± 6%) was achieved (e.g., Fig. 9*C*, left panel) voltage steps elicited only leakage currents that reversed at 0 mV. In parallel with the block of Cl^- current by external NPPB and IAA-94, the block by DDF was evident only when it was added to the bath. That is, the presence of 100 μM intracellular DDF (3/3 cells) did not affect the rate of buildup or maximum amplitude of Cl^- current (e.g., Fig. 9*C*, right panel) but 100 μM external DDF rapidly reduced the current. Proof that verapamil and DDF entered cells readily from the pipette was that in several cells tested with K^+ in the pipette, both drugs blocked the voltage-dependent K^+ current in a use-dependent manner within 30 sec of achieving the whole-cell configuration.

To test for a possible role for the Cl^- channels in T-cell proliferation, we added flufenamic acid, NPPB, IAA-94 or DIDS to suspensions of human T cells 15 min before adding the mitogen, phytahemagglutinin (PHA). In these initial studies we chose a single concentration of each drug that produced 95–100% block of the Cl^- current. Figure 10 shows one representative experiment in which all four Cl^- channel blockers significantly inhibited PHA-induced lymphocyte proliferation. From six such experiments (three replicates each), inhibition was 77 ± 10% (DIDS, 200 μM), 99 ± 1% (flufenamic acid, 200 μM), 94 ± 1% (IAA-94, 400 μM) and 95 ± 2% (NPPB, 200 μM). These blockers did not kill the cells and we (D.J. Phipps and L.C. Schlichter) are now examining their effects on signaling pathways downstream of the T-cell receptor.

Discussion

Small-conductance Cl^- channels have recently been characterized from whole-cell currents in a wide variety of cell types, including immune cells; i.e., normal or leukemic T lymphocytes (Lewis et al., 1993; *present study*), rat mast cells (Matthews et al., 1989) and human neutrophils (Stoddard et al., 1993). Similar channels are likely to underlie the swelling-induced Cl^- currents seen in many cells such as secretory (chromaffin) cells (Doroshenko & Neher, 1992), human endothelial cells (Nilius et al., 1994), and epithelial cells (Botchkin & Matthews, 1993; Diaz et al., 1993). Many of the biophysical, pharmacological and regulatory properties of these Cl^- currents have not been delineated for each cell type and the main research emphasis has been on the volume sensitivity of these Cl^- currents. Nevertheless, it is possible to compare several properties of the current in normal human T lymphocytes (*present study*) with those in different cells.

Biophysical Properties

General features of ion selectivity seem to be conserved among the related Cl^- currents in the cells listed previously. That is, good selectivity of anions over cations, similar halide permeability sequences ($I^- \geq Br^- \geq Cl^- > F^-$, Diaz et al., 1993; Lewis et al., 1993; Stoddard et al., 1993; *present study*) and finite permeabilities to large anions including gluconate and aspartate (usually 0.1–0.2 as permeant as Cl^-, Cahalan & Lewis, 1988; Doroshenko et al., 1991; Valverde et al., 1992; Botchkin & Matthews, 1993; *present study*). One consequence of the relatively poor selectivity of these channels among an-

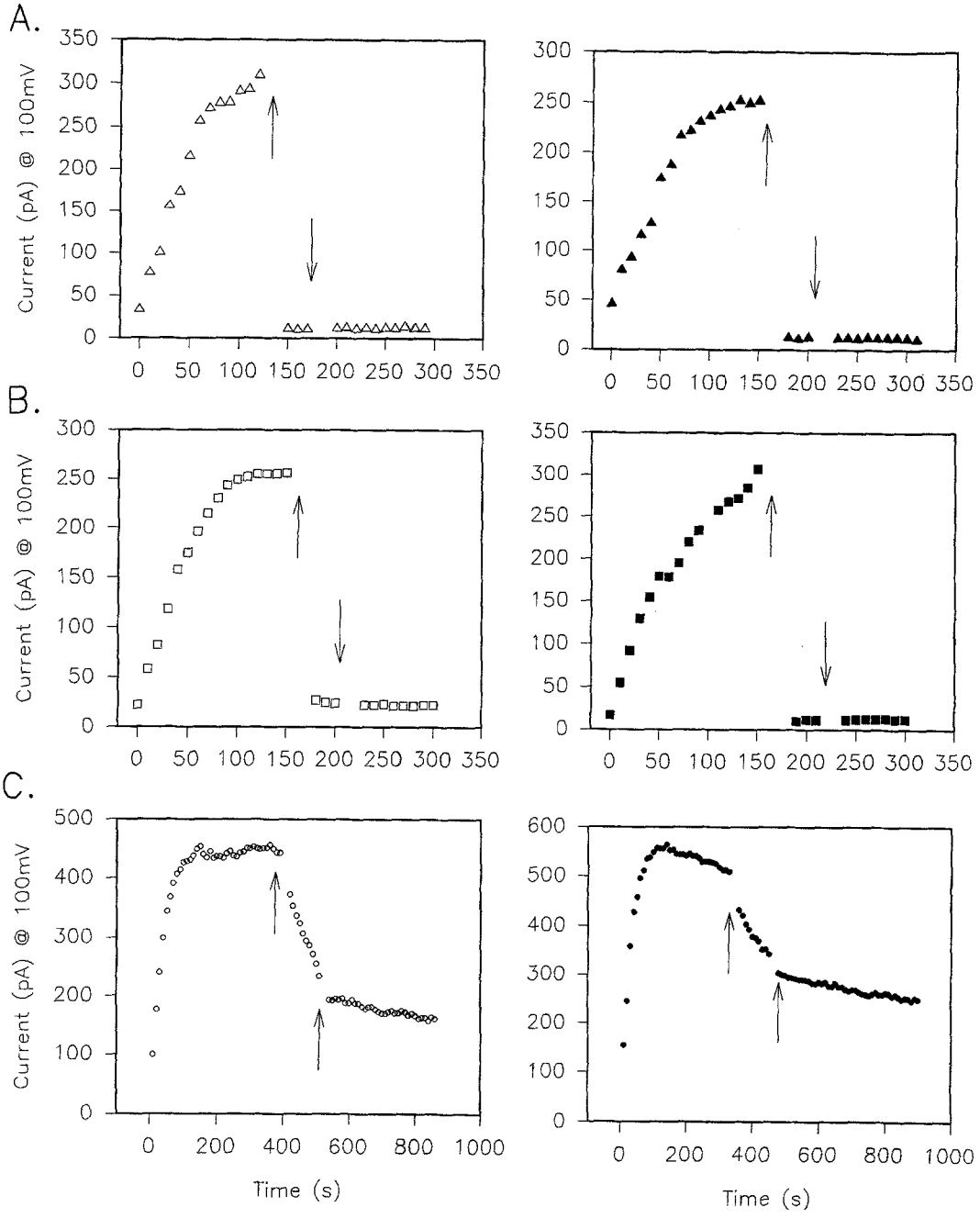

Fig. 9. Acute inhibition of the Cl^- current by externally applied NPPB, IAA-94 and 1,9-dideoxyforskolin. (*A*) 100 μM NPPB; (*B*) 250 μM IAA-94; (*C*) 100 μM 1,9-dideoxyforskolin. For each pair of figures, the left-hand trace shows acute addition of drug to the bath solution (first arrow) then perfusion of the bath with drug-free saline (second arrow). Complete bath exchange took ≈ 40 sec. Each right-hand trace is a different cell in which the pipette-filling solution contained the drug. Then, during the long-lasting plateau phase, the same concentration of drug was applied externally (first arrow) then washed out of the bath (second arrow). The bath saline was 140 mM nMDGCl and the pipette contained 50 mM nMDGCl saline.

ions (compared, for example, to the exquisite selectivity of most K^+ channels over Na^+) is that anion substitution experiments to test functional roles for these channels may give equivocal results, e.g., determining the contribution of Cl^- channels to the resting membrane potential. In addition, an understudied area is the permeability of these channels to physiologically relevant anions including NO_3^-, HCO_3^-, phosphates and sulfates and the possible role of these channels in pH regulation, cellular metabolism and amino acid transport.

A feature of these Cl^- channels that is generally shared among the whole-cell currents in different cell types, is the lack of voltage-dependent gating. Steps of voltage generate currents that show little or no activation

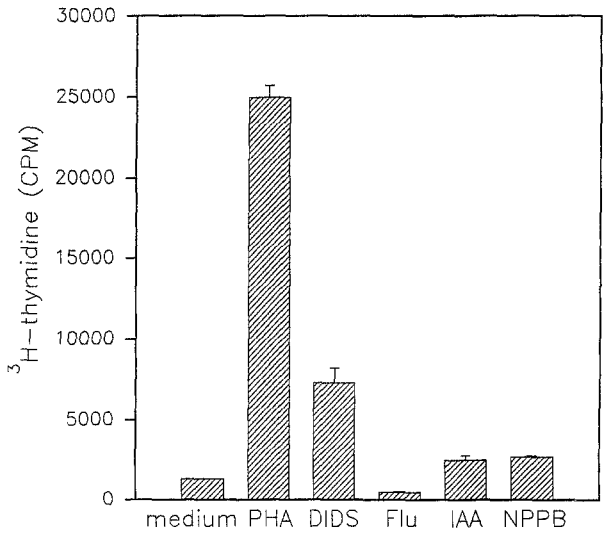

Fig. 10. Chloride channel blockers inhibit lymphocyte proliferation. 2 $\times 10^5$ human T lymphocytes were treated with chloride channel blockers DIDS (200 μM), flufenamic acid (Flu, 200 μM), IAA-94 (IAA, 400 μM) and NPPB (200 μM) in complete cell culture medium, 37°C for 15 min prior to addition of PHA (5 μg/ml). Control cultures were treated with either medium alone (no proliferation) or medium plus PHA (no channel blockers) (100% proliferation). Cells were cultured for 72 h and proliferation was measured as ^{3}H-thymidine incorporation during the final 15 hr of culture. One representative experiment (three replicates) is shown and significant differences were seen ($P < 0.001$) between proliferation in the absence of all chloride channel blockers.

or inactivation kinetics (*see* Fig. 1) once the current has developed in response to cell swelling (e.g., Cahalan & Lewis, 1988; Doroshenko & Neher, 1992; Valverde et al., 1992; Botchkin & Matthews, 1993; Stoddard et al., 1993; Nilius et al., 1994), or following GTPγS diffusion into the cell (Matthews et al., 1989; Doroshenko et al., 1991) or spontaneously (*present study*). At very positive voltages (≥+80 mV) the currents in some cells decrease slowly (e.g., Valverde et al., 1992; Diaz et al., 1993; Nilius et al., 1994), but it is not known if this is a voltage-dependent inactivation or channel block; e.g., internal Mg^{2+} can inhibit the Cl^- current (Stoddard et al., 1993).

In several studies of similar whole-cell Cl^- currents, fluctuation analysis has been used to estimate the single-channel conductance, usually by measuring current variance as a function of mean current, yielding values of 1–2 pS (Matthews et al., 1989; Doroshenko et al., 1991; Lewis et al., 1993; Stoddard et al., 1993; Nilius et al., 1994). Two channel open times could arise from the same Cl^- channel or from the existence of two types of channel, both with very small single-channel conductances. Although it is not possible to rule out either model, the observed enhancement of the whole-cell Cl^- current in these cells by GTPγS (Schlichter et al., 1994) as well as in other cells (e.g., Matthews et al., 1989; Doroshenko et al., 1991; Nilius et al., 1994) suggests that the channels can exist in more than one biochemical state. Whether this regulation corresponds with a change in mean open time may be worth investigating in future.

Among the recently cloned Cl^- channels (ClC0, 1,2,3) the most similar seems to be ClC3. This transcript, when cloned from rat kidney and expressed in XENOPUS oocytes (Kawasaki et al., 1994) produced a Cl^- current that was not voltage-dependent, was outwardly rectified, showed similar anion selectivity to the lymphocyte channel ($I > Cl \approx Br >$ gluconate) and was blocked by a very high DIDS concentration but not by 9-AC or DPC. ClC3 was inhibited by active phorbol esters (Kawasaki et al., 1994), as was the Cl^- current in T lymphocytes (Schlichter et al., 1994). Another intriguing possibility is that the lymphocyte Cl^- channel is ClC-1, which is physically linked to the T-cell receptor β locus (Koch et al., 1992) and codes for a small-conductance Cl^- channel (Pusch, Steinmeyer & Jentsch, 1994). However, ClC-1 channels are blocked by external iodide and 9-AC and close with hyperpolarization below –50 mV, features that differ from the Cl^- current in T lymphocytes.

Channel Regulation and Pharmacology

Most of the Cl^- currents under discussion here build up over tens to hundreds of seconds, either spontaneously after break-in to the whole-cell configuration or after stimulation; e.g., osmotic shock or GTP diffusion into the cell. Many, but not all of the Cl^- currents exhibit swelling sensitivity; for example, the Cl^- current in rat mast cells did not respond to swelling (Penner, Matthews & Neher, 1988; Matthews et al., 1989) and the current in the present study could be slightly reduced by cell shrinkage but not increased by cell swelling. The view that this and similar Cl^- channels are not simply volume sensors is supported by several studies. Pharmacological studies have implicated lipoxygenase products of arachidonic acid metabolism in regulating the Cl^- current in chromaffin and endothelial cells: the PLA_2 inhibitor nordihydroguaiaretic acid (NDGA) blocked Cl^- current induction by either a pressure pulse or GTPγS (Doroshenko et al., 1991; Doroshenko & Neher, 1992; Nilius et al., 1994). Thus, the induction of the Cl^- current in those cells may result from second messenger pathways activated as a consequence of cell swelling.

We tested several compounds that are known Cl^- channel inhibitors in other cells. NPPB blocks the related Cl^- channel in mast cells (10 μM, Matthews et al., 1989), HeLa cells (100 μM, Diaz et al., 1993), and NIH 3T3 cells (Valverde et al., 1992). Both NPPB and the unrelated compound, IAA-94 ([6,7-dichloro-2-cyclopentyl-2,3-dihydro-2-methyl-1-oxo-1H-inden-5-yl)oxy] acetic acid) are such potent blockers of a Cl^- channel in epithelia that they have been successfully used to isolate the channels (Landry et al., 1989). The sensitivity of

similar Cl^- channels to SITS and DIDS seems to differ among cell types and even between authors. For example, 100 μM DIDS (or SITS) blocked the Cl^- current in HeLa cells (Diaz et al., 1993). NIH 3T3 fibroblasts (Valverde et al., 1992) and retinal pigment epithelial cells (Botchkin & Matthews, 1993). Lower DIDS concentrations effectively blocked the current in chromaffin cells (10 μM, Doroshenko et al., 1991), mast cells (10 μM, Matthews et al., 1989) and Jurkat leukemic T cells (<20 μM, Lewis et al., 1993). The regulatory volume decrease (RVD) in human T cells is inhibited by gadolinium (Gd^{3+}) at concentrations as low as 1 μM (Deutsch & Lee, 1988) an effect that cannot be alleviated by gramicidin. This result led Deutsch and Lee (1988) to speculate that the Cl^- channel (rather than the K^+ channel), is blocked by Gd^{3+}; however, we found no block of the small conductance Cl^- channels by up to 100 μM Gd^{3+}.

Possible Physiological Roles

Is the Cl^- conductance described in the present study of peripheral T lymphocytes the same as that characterized by Lewis et al. (1993)? We have no reason to suspect that a different channel protein (gene product) accounts for the differences we have observed. It seems more likely that experimental conditions or cell differences influence channel regulation. Where biophysical comparisons can be made between the present study and that of Lewis et al. (1993) there are strong similarities; i.e., in single-channel conductance, ion selectivity, outward rectification and lack of voltage dependence. Because our work on regulation of this channel (Schlichter et al., 1994 and *unpublished results*) suggests multiple regulatory pathways (PKC, PKA, G proteins), even the choice of pipette-filling solution might influence the spontaneous-*vs.*-swelling-induced development of the current. In this regard, our filling solutions were always of low ionic strength compared with Lewis et al. (1993). Under these conditions we have not seen the exquisite, reversible volume sensitivity reported by Lewis et al. (1993).

We would like to emphasize the possibility that this, and similar, Cl^- conductances may play roles in cells that are not related to volume regulation. Perhaps the apparent variety of effects of second messengers in different cell types reflects different tissue-specific physiological functions of the Cl^- currents. Doroshenko et al. (1991) have suggested that agonist-induced activation of G proteins could alter the electrical excitability of chromaffin cells, potentially altering catecholamine secretion. Penner et al. (1988) proposed that the simultaneous induction of Ca^{2+} and Cl^- conductive pathways following exposure of mast cells to secretagogues provides both a route for the Ca^{2+} influx (Ca channels) and a driving force (via Cl^- channels) for Ca^{2+} influx by maintaining a negative membrane potential, near E_{Cl} (Penner et al., 1988; Matthews et al., 1989). DIDS has been reported to reduce the Ca^{2+} influx necessary for T-cell activation following stimulation by antibodies to the CD3/T-cell receptor complex (Rosoff et al., 1988). Removal of extracellular Cl^- had the same effect, suggesting that DIDS acts on a Cl^- transport pathway. SITS and DIDS inhibit killing by cytotoxic T cells (Gray & Russell, 1986) and natural killer cells (L.C. Schlichter, *unpublished results*) apparently by blocking delivery of the lethal hit (Gray & Russell, 1986). Again, removal of extracellular Cl^- had the same effect. It is tempting to speculate from our data that the Cl^- current in human T cells plays a similar role during T-cell activation; namely, that the sustained rise in $[Ca^{2+}]_i$ during T-cell activation is facilitated by an increased permeability to Cl^-, thus maintaining a negative membrane potential. In this regard, it is interesting that at 37°C immediately upon break-in, there was a significant amplitude of Cl^- current; i.e., ≈40% of the fully activated current. Hence, it is possible that resting T cells express low levels of Cl^- current, which would be expected to mediate a continual Cl^- efflux since the resting potential is more negative than the Cl^- equilibrium potential. We are presently studying the effects of Cl_o and Cl^--channel blockers on different events in T-cell activation, including Ca_i signaling.

We are grateful to Dr. P.S. Pennefather for helpful discussions and comments on this manuscript. Supported by grants to L.C.S. from the Medical Research Council and the National Cancer Institute of Canada and an Ontario Graduate Scholarship to P.A.S.

References

Botchkin, L., Matthews, G. 1993. Chloride current activated by swelling in retinal pigment epithelial cells. *Am. J. Physiol.* **265:**C1037–C1045

Cahalan, M.D., Lewis, R.S. 1988. Role of potassium and chloride channels in volume regulation by T lymphocytes. In: Cell Physiology of Blood, Society of General Physiologists' Series, R.B. Gunn and J.C. Parker, editors. Vol. 43, pp. 281–301. Rockefeller University Press, New York

Deutsch, C., Lee, S.C. 1988. Cell volume regulation in lymphocytes. *Renal Physiol. Biochem.* **3-5:**260–276

Diaz, M., Valverde, M.A., Higgins, C.F., Rucareanu, C., Sepulveda, F.V. 1993. Volume-activated chloride channels in HeLa cells are blocked by verapamil and dideoxyforskolin. *Pfleugers Arch.* **422:**347–353

Diamond, J.M., Wright, E.M. 1969. Biological membranes: The physical basis of ion and nonelectrolyte selectivity. *Rev. Physiol.* **31:**581–647

Doroshenko, P., Neher, E. 1992. Volume-sensitive chloride conductance in bovine chromaffin cell membrane. *J. Physiol.* **449:**197–218

Doroshenko, P., Penner, R., Neher, E. 1991. Novel chloride conductance in the membrane of bovine chromaffin cells activated by intracellular GTPγS. *J. Physiol.* **436:**711–724

Gray, L.S., Russell, J.H. 1986. Cytolytic T lymphocyte effector function requires plasma membrane chloride flux. *J. Immunol.* **136:**3032–3037

Kawasaki, M., Uchida, S., Monkawa, T., Miyawaki, A., Mikoshiba, K.,

Marumo, F., Sasaki, S. 1994. Cloning and expression of a protein kinase C-regulated chloride channel abundantly expressed in rat brain neuronal cells. *Neuron* **12:**597–604

Koch, M.C., Steinmeyer, K., Lorenz, C., Ricker, K., Wolf, F., Otto, M., Zoll, B., Lehmann-Horn, F., Grzeschik, K-H, Jentsch, T.J. 1992. The skeletal muscle chloride channel in dominant and recessive human myotonia. *Science* **257:**797–800

Krapivinsky, G.B., Ackerman, M.J., Gordon, E.A., Krapivinsky, L.D., Clapham, D.E. 1994. Molecular characterization of a swelling-induced chloride conductance regulatory protein, pI_{Cln}. *Biophys. J.* **66(2):**A167

Landry, D.W., Akabas, M.H., Redhead, C., Edelman, A., Cragoe, E.J., Al-Awqati, Q. 1989. Purification and reconstitution of chloride channels from kidney and trachea. *Science* **244:**1469–1472

Lewis, R.S., Ross, P.E., Cahalan, M.D. 1993. Chloride channels activated by osmotic stress in T lymphocytes. *J. Gen. Physiol.* **101:**801–826

Mathias, R.T., Cohen, I.S., Oliva, C. 1990. Limitations of the whole cell patch clamp technique in the control of intracellular concentrations. *Biophys. J.* **58:**759–770

Matthews, G., Neher, E., Penner, R. 1989. Chloride conductance activated by external agonists and internal messengers in rat peritoneal mast cells. *J. Physiol.* **418:**131–144

Nilius, B., Oike, M., Zahradnik, I., Droogmans, G. 1994. Activation of a Cl^- current by hypotonic volume increase in human endothelial cells. *J. Gen. Physiol.* **103:**787–805

Pahapill, P.A., Schlichter, L.C. 1990. Modulation of potassium channels in human T lymphocytes: effects of temperature. *J. Physiol.* **422:**103–126

Pahapill, P.A., Schlichter, L.C. 1992*a*. Cl^- channels in intact human T lymphocytes. *J. Membrane Biol.* **125:**171–183

Pahapill, P.A., Schlichter, L.C. 1992*b*. Modulation of potassium channels in intact human T lymphocytes. *J. Physiol.* **445:**407–430

Paulmichl, M., Li, Y., Wickman, K., Ackerman, M., Peralta, E., Clapham, D. 1992. New mammalian chloride channel identified by expression cloning. *Nature* **356:**238–241

Penner, R., Matthews, G., Neher, E. 1988. Regulation of calcium influx by second messengers in rat mast cells. *Nature* **334:**499–504

Pusch, M., Steinmeyer, K., Jentsch, T.J. 1994. Low single-channel conductance of the major skeletal muscle chloride channel, CIC-1. *Biophys. J.* **66:**149–152

Rosoff, P.M., Hall, C., Gramates, L.S., Terlecky, S.R. 1988. 4,4′-diisothio-cyanatostilbene-2,2′-disulphonic acid inhibits CD3-T cell antigen receptor-stimulated Ca^{2+} influx in human T lymphocytes. *J. Biol. Chem.* **263:**19535–19540

Sarkadi, B., Parker, J.C. 1991. Activation of ion-transport pathways by changes in cell volume. *Biochim. Biophys. Acta.* **1071:**407–427

Schlichter, L.C., Grygorczyk, R., Pahapill, P.A., Grygorczyk, C. 1990. A large, multiple-conductance Cl^- channel in normal human T lymphocytes. *Pfleugers Arch.* **416:**413–421

Schlichter, L.C., Schumacher, P.A., Sakellaropoulos, G. 1994. Are small conductance Cl^- channels shape and volume sensors? *Biophys. J.* **66(2):**A168

Stoddard, J.S., Steinbach, J.H., Simchowitz, L. 1993. Whole cell Cl^- currents in human neutrophils induced by cell swelling. *Am. J. Physiol.* **265:**C156–C165

Valverde, M.A., Diaz, M., Sepulveda, F.V., Gill, D.R., Hyde, S.C., Higgins, C.F. 1992. Volume-regulated chloride channels associated with the human multidrug-resistance P-glycoprotein. *Nature* **322:**467–470